Supplementary Information (SI) for RSC Advances.

Supporting Information

Mitigating Interfacial Reactions in $Li_4Ti_5O_{12}$ Anodes through Carbon Shells Synthesized by Spray Granulation

Dong-Ze Wu[a, b], Wen-Chia Hsu[c], Chia-Huan Chung[b, d], Hsin-Yu Hsieh[b], Wei-Ming Chen[b], Feng-Yu Wu[b], Yu-Hsuan Su[b], Hwai-En Lin[e], Maw-Kuen Wu[b], Phillip M. Wu[b]*, Yu-Cheng Chiu[a, f, g]*, and Po-Wei Chi[b, h]*

[a] Graduate Institute of Energy and Sustainability Technology, National Taiwan University of Science and Technology, 43 Keelung Road, Sec 4, Taipei 10607, Taiwan

[b] Institute of Physics, Academia Sinica, 128, Section 2, Academia Road, Taipei 11529, Taiwan

[c] GUS Technology, Taoyuan City, 32063, Taiwan

[d] Graduate Institute of Applied Science and Technology, National Taiwan University of Science and Technology, 43 Keelung Road, Sec 4, Taipei 10607, Taiwan

[e] Department of Mechanical Engineering, College of Mechanical & Electrical Engineering, National Taipei University of Technology (TAIPEI TECH), 1, Section 3, Zhongxiao E. Rd., Taipei 106, Taiwan

[f] Department of Chemical Engineering, National Taiwan University of Science and Technology, 43 Keelung Road, Sec 4, Taipei 10607, Taiwan

[g] Sustainable Electrochemical Energy Development Center, National Taiwan University of Science and Technology, Taipei City 106, Taiwan

[h] Department of Mechanical Engineering, Chung Yuan Christian University 200, Chungpei Road, Chungli District, Taoyuan City 32023, Taiwan

*Corresponding author

ycchiu@mail.ntust.edu.tw

pmwu429@gate.sinica.edu.tw

poweichi@gate.sinica.edu.tw/pwchi@cycu.edu.tw

Table S1. Lattice parameters of LC0, LC5, LC7.5, and LC10.

Sample	*a* (Å)	V (Å^3)	R profile
LC0	8.358	583.9	4.50
LC5	8.357	583.8	4.18
LC7.5	8.357	583.8	4.59
LC10	8.358	583.9	4.37

Table S2. Particle size distribution and Zeta potential of LC0, LC5, LC7.5, and LC10.

Sample	D10 (μm)	D50 (μm)	D90 (μm)	Zeta Potential (mV)
LC0	4.36	8.14	13.76	65.04±1.5
LC5	5.14	8.24	12.93	-63.03±1.5
LC7.5	5.27	8.73	13.98	-55.57±1.5
LC10	5.16	8.73	14.13	-61.03±2

The zeta potentials of all samples were measured using an electrophoretic light scattering spectrophotometer (ELS-2000, Otsuka Electronics Co., Osaka, Japan). A dispersion of 0.05 g of LTO and LTO@C in 15 ml deionized water was prepared in a quartz cell to determine the electrophoretic mobility.

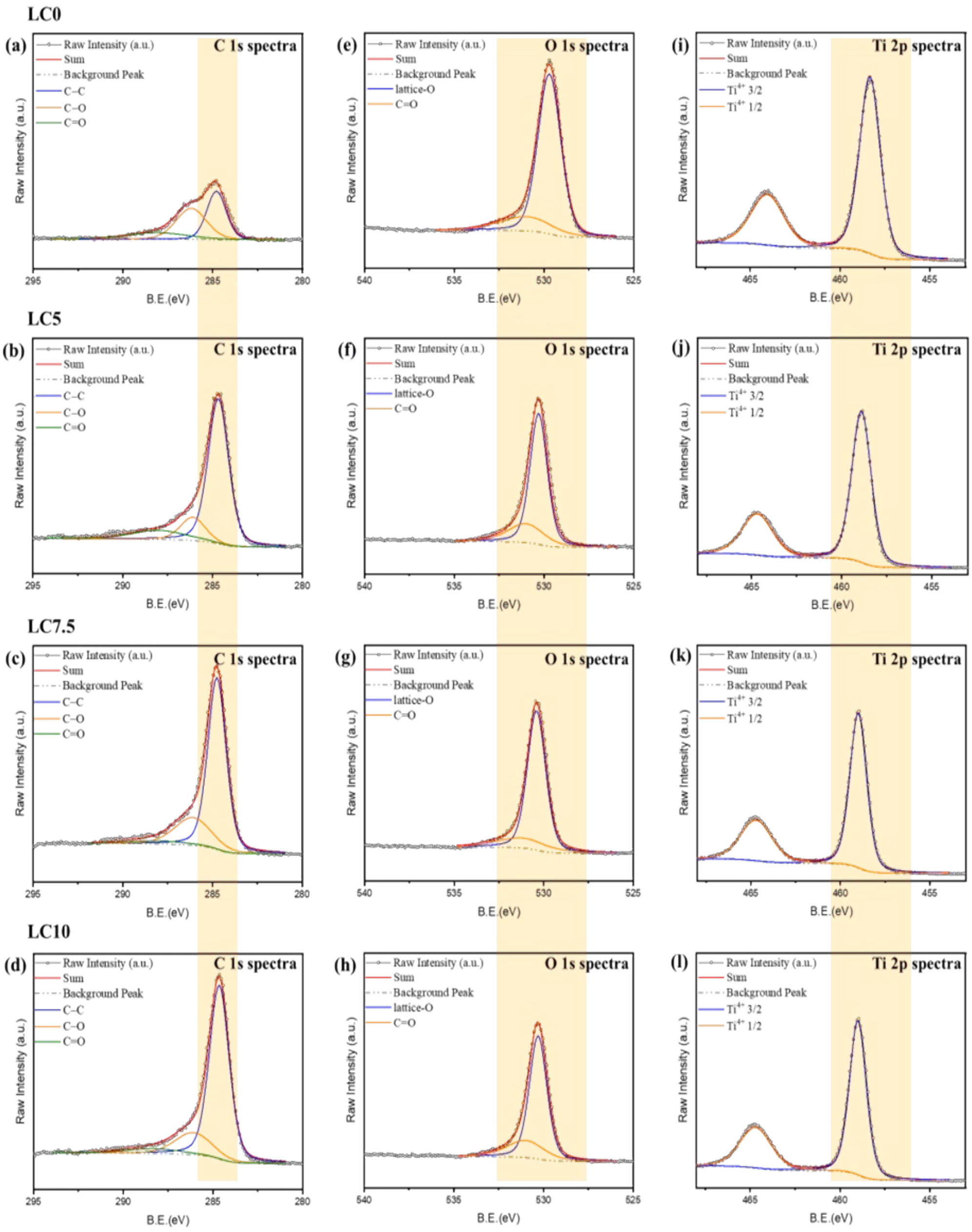

Figure S1. (a-d) C 1s, (e-h) O 1s, and (i-l) Ti 2p XPS spectra of LC0, LC5, LC7.5, and LC10 powders.

We employed XPS analysis to investigate the differences in the C 1s, O 1s, and Ti 2p core-level spectra of the LTO and LTO@C powders, as shown in **Figure S1**. Obviously, the core-level spectra of LTO@C exhibited changes with increasing sucrose concentrations (5%, 7.5%, and 10%) following carbon coating. In the C 1s spectrum (**Figures S1 (b)-(d)**), the C-C signal intensity gradually increased due to the carbon coating, which also influenced the O 1s and Ti 2p spectra. The lattice oxygen signal intensity in the O 1s and Ti 2p spectra of LTO@C significantly decreased due to the carbon coating, with the signal peaks shifting to higher binding energies. **[1]**

As shown in **Figures S1 (a)**, **(e)**, and **(i)**, the C 1s spectrum of LTO powder showed signals at 284.8 eV (C-C), 286.1 eV (C-O), and 289 eV (C=O). The C-C signal mainly originates from adventitious carbon, while C=O is contributed by the residual Li_2CO_3 on the surface. In the O 1s spectrum, the signal at 529.8 eV mainly corresponds to the lattice oxygen of LTO, while the signal at 531 eV (C=O) is attributed to Li_2CO_3. The Ti 2p spectrum consists of a doublet of peaks located at 458.3 eV and 464 eV, corresponding to the Ti^{4+} ion of LTO. **[2, 3]**

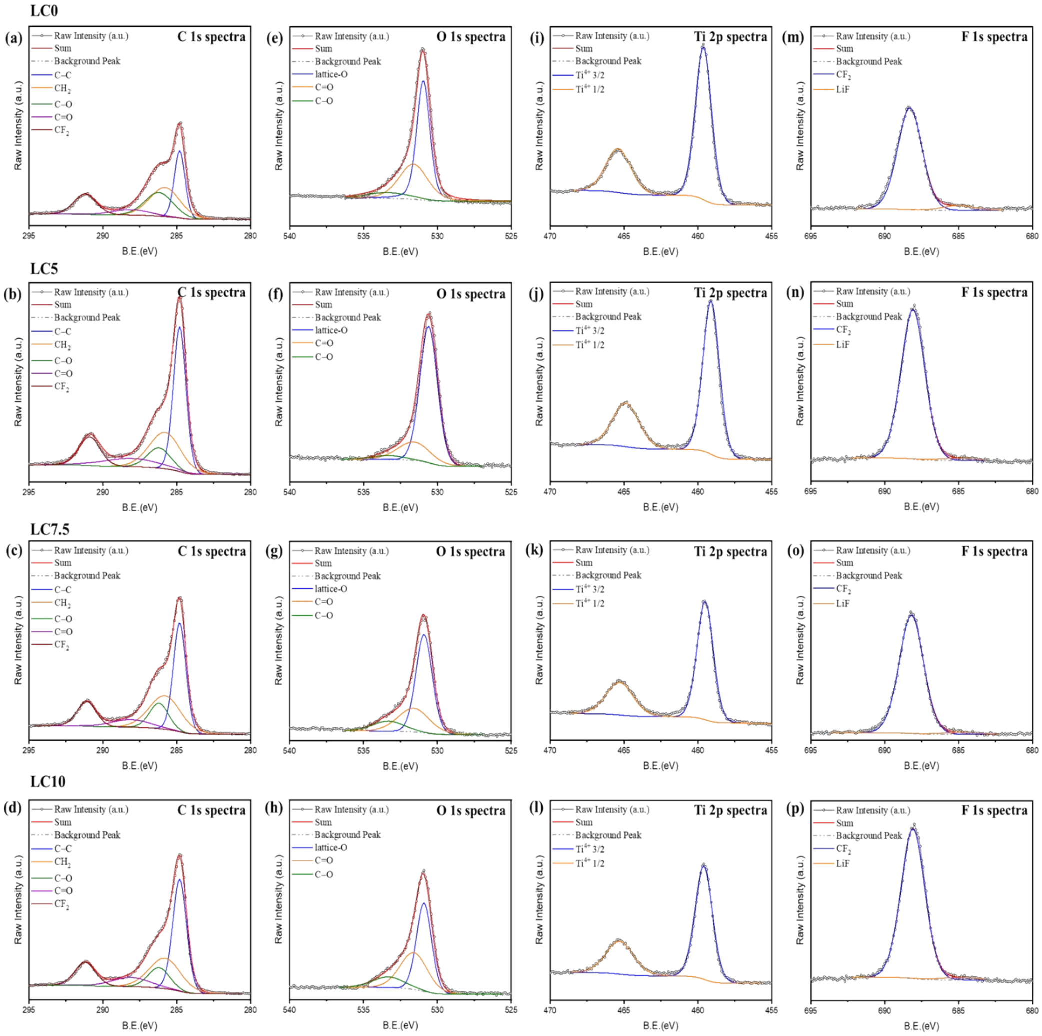

Figure S2. The XPS spectra of the LC0, LC5, LC7.5, and LC10 electrodes before 200 cycles. (a-d) C 1s, (e-h) O 1s, (i-l) Ti 2p, and (m-p) F 1s regions.

Figure S2 presents the XPS spectra of the LC0, LC5, LC7.5, and LC10 electrodes. The C 1s spectra reveal additional signals at 285.7 eV (CH_2) and 291 eV (CF_2) beyond those observed from the powder, attributed to the PVDF binder. The (C-C) signal also includes contributions from carbon black (Super P). The O 1s and Ti 2p spectra remained largely unchanged compared to those of the powder. In the F 1s spectra, signals at 685 eV (LiF) and 688 eV (CF_2) were detected, with the CF_2 signal originating from PVDF and the small LiF peak likely resulting from surface contamination during sample preparation. **[4-7]**

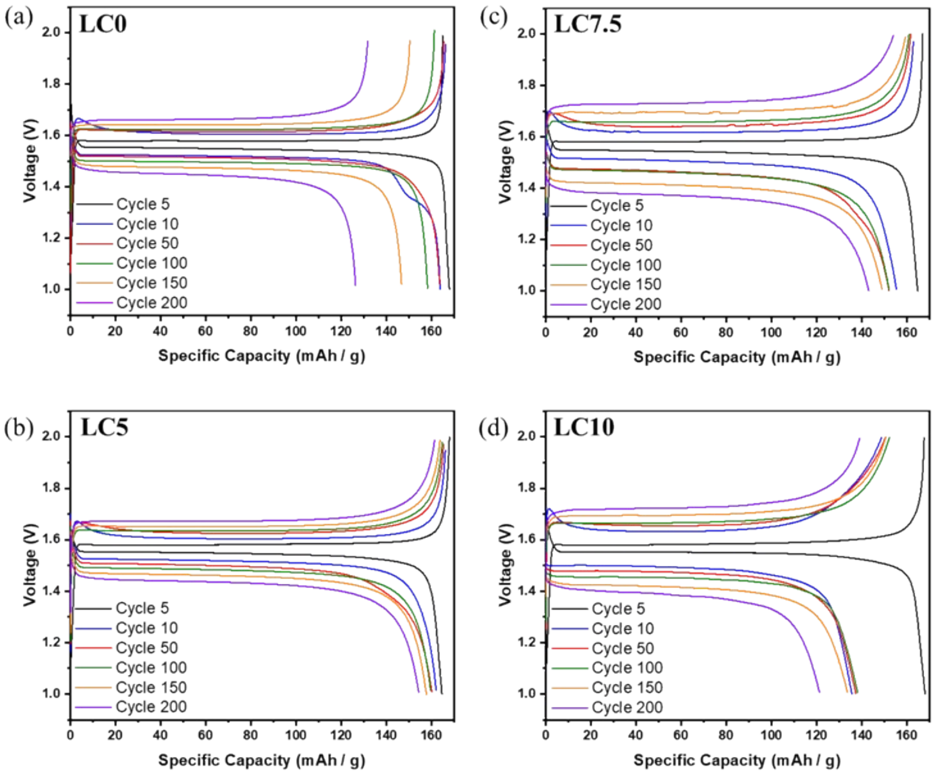

Figure S3. Charge-discharge curves (a) LC0, (b) LC5, (c) LC7.5, and (d) LC10 under 1C with potential range examined from 1 V to 2 V.

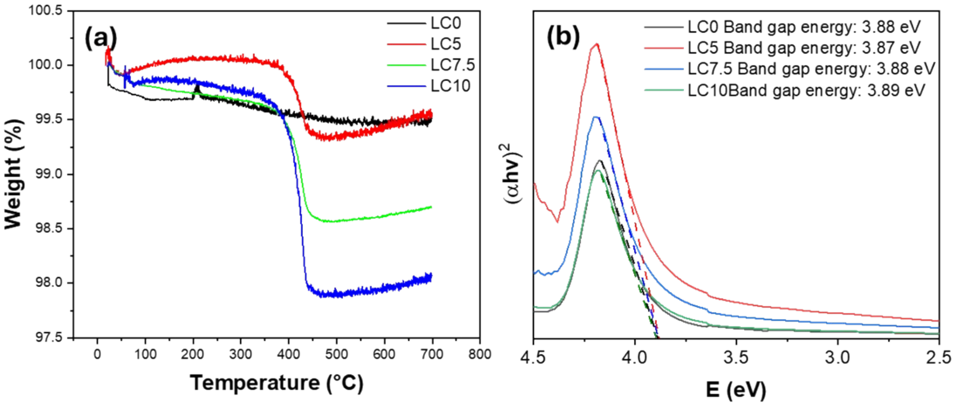

Figure S4. (a) TGA curves of LC0, LC5, LC7.5, and LC10 powders. (b) Tauc plots of LC0, LC5, LC7.5, and LC10 samples derived from UV-Vis reflectance spectra.

References

[1] S. J. Rezvani *et al.*, "Binder-Induced Surface Structure Evolution Effects on Li-Ion Battery Performance." Appl. Surf. Sci., vol. 435, 2018, pp. 1029–1036.

[2] R. T. Haasch *et al.*, "Lithium-Based Transition-Metal Oxides for Battery Electrodes Analyzed by X-Ray Photoelectron Spectroscopy. X. $Li_4Ti_5O_{12}$." Surf. Sci. Spectra, vol. 26, 2019, 014012.

[3] D. V. Pelegov *et al.*, "Efficiency Threshold of Carbon Layer Growth in $Li_4Ti_5O_{12}$/C Composites." J. Electrochem. Soc., vol. 166, no. 3, 2019, A5019-A5024.

[4] Y. He *et al.*, "Gassing in $Li_4Ti_5O_{12}$-Based Batteries and Its Remedy." Sci. Rep., vol. 2, 2012, article 913.

[5] J. Gieu *et al.*, "Influence of Vinylene Carbonate Additive on the $Li_4Ti_5O_{12}$ Electrode/Electrolyte Interface for Lithium-Ion Batteries." J. Electrochem. Soc., vol. 164, no. 6, 2017, A1314-A1320.

[6] S. Malmgren *et al.*, "Comparing Anode and Cathode Electrode/Electrolyte Interface Composition and Morphology Using Soft and Hard X-Ray Photoelectron Spectroscopy." Electrochim. Acta, vol. 97, 2013, pp. 23–32.

[7] R. Dedryvère *et al.*, "Electrode/Electrolyte Interface Reactivity in High-Voltage Spinel $LiMn_{1.6}Ni_{0.4}O_4$/$Li_4Ti_5O_{12}$ Lithium-Ion Battery." J. Phys. Chem. C, vol. 114, 2010, pp. 10999–11008.